Available online at BCREC website: https://bcrec.id

Bulletin of Chemical Reaction Engineering & Catalysis, 15 (2) 2020, 476-489

Research Article

Effective TiO_2-Sulfonated Carbon-derived from *Eichhornia crassipes* in The Removal of Methylene Blue and Congo Red Dyes from Aqueous Solution

Iis Intan Widiyowati[1], Mukhamad Nurhadi[1,*], Muhammad Hatami[1], Lai Sin Yuan[2,3]

[1]*Department of Chemical Education, Universitas Mulawarman, Kampus Gunung Kelua, Samarinda, 75123, East Kalimantan, Indonesia.*
[2]*School of Energy and Chemical Engineering, Xiamen University Malaysia, Selangor Darul Ehsan 43900, Malaysia.*
[3]*College of Chemistry and Chemical Engineering, Xiamen University, Xiamen 361005, China.*

Received: 4th January 2020; Revised: 26th May 2020; Accepted: 27th May 2020; Available online: 30th July 2020; Published regularly: August 2020

Abstract

The study of TiO_2-sulfonated carbon-derived from *Eichhornia crassipes* (TiO_2/SCEC), as an effective adsorbent to remove Methylene blue (MB) and Congo red (CR) dyes from aqueous solution, has been conducted. The preparation steps of TiO_2/SCEC adsorbent involved the carbonisation of *E. crassipes* powder at 600 °C for 1 h, followed by sulfonation of carbon for 3 h and impregnation through titanium(IV) isopropoxide (500 µmol). The physical properties of the adsorbents were characterized by using X-ray fluorescence (XRF), Fourier transform infrared, X-ray diffraction (XRD), Scanning electron microscopy with Energy dispersive X-ray (SEM-EDX), Thermogravimetric analysis (TGA) and nitrogen adsorption-desorption studies. The dye removal study using TiO_2/SCEC adsorbent was carried out by varying of contact time, adsorbent dosage, initial dye concentration, pH, particles size of adsorbent and temperature. The kinetics models were determined by the effects of contact time and the thermodynamic parameters (ΔH, ΔS, and ΔG), which were calculated by the effects of temperature. The results showed that the maximum dye removal capacity of TiO_2/SCEC were 18.8 $mg.g^{-1}$ for MB and 36.5 $mg.g^{-1}$ for CR. The removal of MB and CR dyes using TiO_2/SCEC adsorbent performed a pseudo-second order kinetic models with spontaneity. Copyright © 2020 BCREC Group. All rights reserved

Keywords: *Eichhornia crassipes*; TiO_2; methylene blue; congo red; adsorption; carbon

How to Cite: Widiyowati, I.I., Nurhadi, M., Hatami, M., Yuan, L.S. (2020). Effective TiO_2-Sulfonated Carbon-derived from *Eichhornia crassipes* in The Removal of Methylene Blue and Congo Red Dyes from Aqueous Solution. *Bulletin of Chemical Reaction Engineering & Catalysis*, 15(2), 476-489 (doi:10.9767/bcrec.15.2.6997.476-489)

Permalink/DOI: https://doi.org/10.9767/bcrec.15.2.6997.476-489

1. Introduction

Synthetic dyestuff like Methylene blue (MB) and Congo red (CR) are very dangerous for human and animal life if discharged into the environment. Synthetic dyestuff seldom are removed as liquid waste in large volumes from many industries [1]. Liquid waste that polluted by Methylene blue (MB) and Congo red (CR) is commonly produced in textile, paint, papers, hair colorant, leather industries. The amount of dyes in the liquid waste from industries depending on many factor such as dyeing methods, type of coloured raw material (type of fabric), as well as type and amount of dyes. The quality of water became decrease with a very small

* Corresponding Author.
E-mail: nurhadi1969@yahoo.co.id (M. Nurhadi);
Telp: +62 81346482251; Fax: +62 541 743929.

amount of synthetic dyestuff (ppm) dissolved in the water, as they affect the colour of water and disqualify it for home and technological purposes. A large number of synthetic dyestuff into the environment can become serious problem due to it causes infertility of the soil, increased amount of chemical oxygen demand in water, and reduced light penetrability that can inhibition the photosynthetic processes [2,3]. Some synthetic dyestuffs have negative effect for living human and organism if their presences in water due to their properties are carcinogenic and mutagenic. Many problems for human health were caused by dyes such as an adverse effect on the functioning of liver, reproductive system, and kidneys, increased heart rate, vomiting, shock, jaundice, chromosomal damage, respiratory enzymes impairment, and the formation of tumors [2,4,5].

Many different methods have been used in removing synthetic dyestuff from wastewater in order to reduce their impacts on the environment. The wastewater treatment methods for removal of pollutants from aqueous solution like photochemical degradation [6], biological degradation [7], chemical oxidation [8], electrocoagulation [9], coagulation and flocculation [10], adsorption [3,11-13], ozonation [14], fungal decolorization [15], have been investigated with varying degree of success. Among of wastewater treatment technologies, adsorption is rapidly gaining prominence as physicochemical method of treating aqueous effluent due its proven efficiency and great potential as means of producing quality effluent [16].

Eichhornia crassipes (water hyacinth) is a weed plant with a high growth rate that can damage the aquatic environment, such as in many tropical lake and river. Its existence can disrupt fisheries, transportation and hydroelectric power production. Several study have been conducted with *E. crassipes* raw material to produce dye adsorbent, such as: *E. crassipes* for removal of azo and anthraquinone dyes from aqueous solution [17], the root of *E. crassipes* for adsorption of Congo red dye from aqueous solution [16], *E. crassipes* for adsorption of Methylene blue dye from aqueous solution [2]. However, the results from the previous research show that the dye removal capacity is low (Q_m = 1.58 mg.g^{-1}) and the amount of adsorbent (1 g, 50 mL of dye solution) that used is not economical.

Here, we report the usage of carbon from *E. crassipes*, which were modified by sulfonation and TiO_2 impregnation, as adsorbent for the removal of Methylene blue and Congo red dyes from aqueous solution. TiO_2 is one of the promising adsorbent widely adopted to adsorb dyes, such as Methylene Blue, Methyl Orange, Malacite Green, Crystal Violet, Thymol Violet, Acid Red G, Reactive Red 195, *etc.*, owing to it is comprised of hydroxyl groups, which could induce electrostatic charge and Van der Waals forces with those dyes [18-22]. However, the hydroxyl groups might be limited for high amount dyes adsorption. Hence, TiO_2 is further modified with carbon source via sulfonation to enhance the adsorption capability. The function of sulfonation process was to enhance the number of oxygen functional groups that can serve as the adsorption sites, while increasing hydrophilicity [23]. The oxygen functional groups onto sulfonated carbon from *E. crassipes* act an importable in uniformly dispersing TiO_2 on the surface and tailoring the particle size of TiO_2, which result in great enhancement of adsorption capacity of dyes due to higher surface area. TiO_2 was impregnated onto sulfonated carbon from *E. crassipes* due to TiO_2 has a high activity to adsorb dyes pollutants in water, low cost, non-toxicity, chemical stability, and environmental friendliness [5,24].

In this research, the dye removal capacity, the effect of contact time, pH, initial concentration of dyes, adsorbent dosage and aqueous solution temperature have been carried out. The adsorption isotherm was checked by using the Freundlich isotherm and the Langmuir isotherm. The maximum dye removal capacity was determined by the Langmuir equation. The kinetics process in the adsorption of MB and CR dyes onto TiO_2-sulfonated carbon-derived from *E. crassipes* were investigated by using Lagergren and Svenska equation. The Van't Hoffs plots were used to investigate the parameter thermodynamic enthalpy, entropy and free energy.

2. Materials and Methods

2.1 Carbonazation Process

The *E. crassipes* from a pool around Mulawarman University were used as raw materials sources. The trunk of *E. crassipes* was washed with tap water to remove impurities. Then, it was cut and dried in oven at 110 °C overnight. The carbon was derived from *E. crassipes* powder after the carbonization process in a furnace at 600 °C for 1 h. The carbon-derived from *E. crassipes* was labeled as CEC.

Copyright © 2020, BCREC, ISSN 1978-2993

2.2 Sulfonation Process

The sulfonation process follows the previous research [23]. Every gram carbon was mixed with 6 mL sulfuric acid (98%, JT Baker) and stirred at room temperature for 3 h. The acid remaining in the sample was washed with distilled water and dried in an oven at 110 °C for overnight. Furthermore, the sulfonated carbon-derived from *E. crassipes* is labeled as SCEC.

2.3 Titania Impregnation

The impregnation process was done by immersing 1 g sulfonated carbon in 10 mL toluene (Merck) containing titanium(IV) isopropoxide (500 μmol, Aldrich) and stirred until all of the toluene solvent completely evaporated. The residual toluene was removed from the sample by washing with ethanol (Merck) and subsequently dried at 110 °C for overnight. Then the sample was calcined at 350 °C for 2 h. The sulfonated carbon which has been impregnated is TiO_2-sulfonated carbon-derived from *E. crassipes* with a denotation of TiO_2/SCEC.

2.4 Samples Characterization

The elemental analysis, the Fourier transform infrared spectroscopy, X-ray diffraction (XRD), thermogravimetric analysis (TGA) and differential thermal analysis (DTA), scanning electron microscopy (SEM), and nitrogen adsorption-desorption studies were used to investigate the properties of TiO_2/SCEC adsorbent. The elemental analysis by X-ray Fluorescence (PANalytical MiniPa 14 type) was used to determine elements contained in the adsorbent. The FTIR spectroscopy (IR−Prestige−21 Shimadzu) was used to determine the functional groups in the adsorbent. Crystallinity and phase content of the sample was investigated by XRD (Phillips PANalytical X'Pert PRO type), with the Cu Kα (λ = 1.5406 Å) radiation. The Thermal Gravimetric Analysis (TGA) data which collected using Linseis Type STA PT1600 instrument with heat rate 10 °C.min^{-1} and target temperature 800 °C was used to determine the amount of carbon in the adsorbent. SEM images which obtained from a FEI Inspect S50 instrument was used to investigate the surface morphology of the adsorbent. The nitrogen adsorption–desorption isotherms, surface area, micropore area and pore size distribution were created from the data which collected from a Quantachrome Nova 1200e instrument.

2.5 Adsorption Test

The performance of adsorbent was tested using Methylene blue ($C_{16}H_{18}ClN_3S.xH_2O$, x = 2-3, Merck) and Congo red ($C_{32}H_{22}N_6O_6S_2$, Merck) dyes. The Methylene blue and Congo red structures were shown in Figure 1. The adsorption was carried out by mixing 0.250 g the adsorbent with 25 mL of MB solution (100 mg.L^{-1}) or 0.125 g adsorbent with 25 mL of CR dye solution (100 mg.L^{-1}) in a 100 mL beaker glass at room temperature for the duration of 5, 10, 15, 20, 25, 30, 60, 120, and 240 min. Furthermore, the adsorbent was separated from the filtrate by centrifugation and the residual dye in the filtrate was analyzed by using UV-Vis spectrophotometer by monitoring the changes in absorbance at 660 nm for MB and 550 nm for CR. The effect of particle size of adsorbent for dye sorption capacity was investigated by varying size such as 40–100; 100–200 and < 200 mesh. The effect of pH was evaluated in the pH range of 2.0–10.0 for MB and 5.0–10.0 for CR dye. The initial pH of dye solution

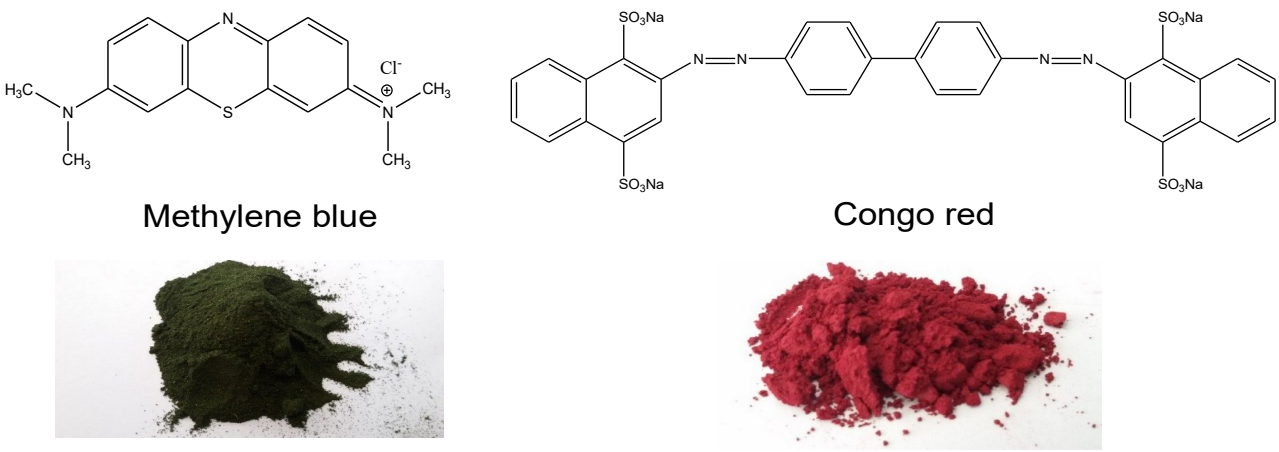

Figure 1. The chemical structure of dyes.

Copyright © 2020, BCREC, ISSN 1978-2993

was fixed by the mixing 0.1 M HCl and 0.1 M NaOH. The effect of initial dye concentration was investigated by varying initial concentrations 100, 200, 300, 400, 500, and 600 mg.L^{-1}. In this study, the thermodynamic parameters (enthalpy, entropy and free energy) also were investigated with follow the adsorption data of the effect of temperature (25, 40 and 50 °C).

The adsorption efficiency of the adsorbent was determined following Equation (1) [16,23].

$$Adsorption\ efficiency\ (\%) = \frac{(C_0 - C_t)}{C_0} \times 100\% \quad (1)$$

where C_0 is the dye initial concentration and C_t is the dye concentration after adsorption time t (mg.L^{-1}) in the solution. The adsorption capacity q_t of adsorbent (mg/g) was calculated with following the equation [25,26]:

$$q_t = \frac{(C_0 - C_t)V}{W} \quad (2)$$

and V is the volume of dye solution (mL) and W is weight adsorbent (g).

The adsorption kinetic of MB and CR adsorption onto TiO_2/SCEC adsorbent were described by the pseudo-first-order kinetic models and the pseudo-second-order kinetic model. The pseudo-first-order kinetic models expression of Lagergren base on the sorption capacity of adsorbent is expressed as [27-29]:

$$\frac{dq_t}{dt} = k_1(q_e - q_t) \quad (3)$$

$$\frac{dq_t}{(q_e - q_t)} = k_1 dt \quad (4)$$

Integration of Equation (4) for the boundary condition $t = 0$ to $t = t$ and $q_t = 0$ to $q_t = t$ can be found the equation:

$$\ln(q_e - q_t) = \ln q_e - k_1 t \quad (5)$$

where k_1 (g/mg.h) is the rate constant for Lagergren pseudo first-order, q_e and q_t are the amounts of dye adsorbed per gram of adsorbent (mg/g) at equilibrium and any time t. The value of k_1 and q_e can be determined from slope and intercept from plot ln (q_e-q_t) versus t.

The pseudo-second-order kinetic model is also based on the sorption capacity of the adsorbent. Linier form of pseudo-second-order kinetic model was expressed by Ho and McKay in Equations (6-7)[30,31]:

$$\frac{dq_t}{dt} = k_2(q_e - q_t)^2 \quad (6)$$

$$\frac{dq_t}{(q_e - q_t)^2} = k_2 dt \quad (7)$$

Integration of Equation (7) for the boundary condition $t = 0$ to $t = t$ and $q_t = 0$ to $q_t = t$ can be found Equation (8).

$$\frac{1}{(q_e - q_t)} - \frac{1}{q_e} = k_2 t \quad (8)$$

Equation (8) was rearranged to obtain:

$$\frac{q_t}{q_e(q_e - q_t)} = k_2 t \quad (9)$$

$$q_t = k_2 q_e^2 t - k_2 q_e q_t \quad (10)$$

Equation (10) was divided by $k_2 q_t q_e^2$ to obtain:

$$\frac{1}{k_2 q_e^2} = \frac{t}{q_t} - \frac{t}{q_e} \quad (11)$$

Rearrangement of equation (11) was obtained:

$$\frac{t}{q_t} = \frac{1}{k_2 q_e^2} + \frac{t}{q_e} \quad (12)$$

where k_2 (g.mg^{-1}.h^{-1}) is the rate constant for pseudo-second-order, q_e and q_t are the amounts of dye adsorbed per gram of adsorbent (mg.g^{-1}) at equilibrium and any time t. The value of k_2 and $q_{e,cal}$ can be calculated from intercept and slope form the plot t versus t/q_t.

The activation energy (E_a) for adsorption process onto TiO_2/SCEC adsorbent was investigated using the Arrhenius equation. The equation is given as [25,32]:

$$\ln k = \ln A - \frac{E_a}{RT} \quad (13)$$

k, E_a (kJ.mol^{-1}), T (K), R (J.mol^{-1}.K^{-1}) and A are the rate constant, Arrhenius activation energy, temperature of the adsorption medium, the ideal gas constant (8.314 J.mol^{-1}.K^{-1}), and the Arrhenius factor, respectively. The Arrhenius activation energy was determined from slope of plotting ln k versus $1/T$.

The adsorption isotherm of adsorption process onto TiO_2/SCEC adsorbent was investigated by the Langmuir and the Freundlich isotherm. The Langmuir isotherm is correlated with monolayer sorption onto a surface. The Langmuir equation is given by [33-35]:

$$\frac{C_e}{q_e} = \frac{1}{Q_{max}} C_e + \frac{1}{Q_{max}.b} \quad (14)$$

where Q_{max} and b are Langmuir constant which correlated with maximum adsorption capacity and bonding energy of adsorption, respectively. The slope and intercept of the linier plot of C_e/q_e versus C_e was used to determine Q_{max} and b.

The Freundlich isotherm model assumes heterogeneous site energies of sorption. The

Copyright © 2020, BCREC, ISSN 1978-2993

Freundlich equation is followed as [25,34]:

$$\ln q_e = \ln K_F + \left(\frac{1}{n}\right)\ln C_e \quad (15)$$

where K_F and n are the Freundlich constant which indicate adsorption capacity and adsorption intensity, respectively. The intercept and slope of the plot of ln q_e versus ln C_e were used to calculated K_F (mg.g^{-1}) and n (L.mg^{-1})$^{1/n}$.

The thermodynamic parameters free energy (ΔG), enthalpy (ΔH) and entropy (ΔS) were determined by the experiments that were created at different temperatures. The value changes of ΔH and ΔS of adsorption were estimated from the following equation [32,36]:

$$\Delta G^0 = -RT \ln K_C \quad (16)$$

$$\Delta G^0 = \Delta H - T\Delta S \quad (17)$$

The correlation of equation (16) and (17) was obtained:

$$-RT \ln K_C = \Delta H - T\Delta S \quad (18)$$

Equation (18) was arranged to obtain Van't Hoff equation:

$$\ln K_C = -\frac{\Delta H}{R}\frac{1}{T} + \frac{\Delta S}{R} \quad (19)$$

with K_C is the equilibrium constant which calculated by the equation:

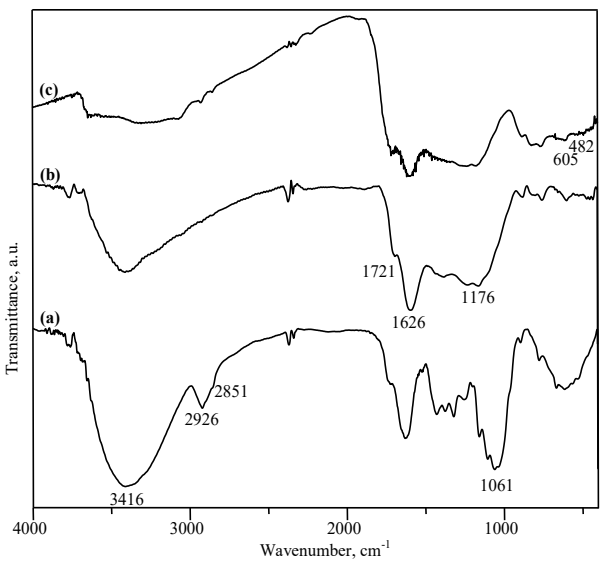

Figure 2. FTIR spectra of (a) CEC, (b) SCEC and (c) TiO_2/SCEC adsorbent.

$$K_C = \frac{C_1}{C_2} \quad (20)$$

where T, R, C_1 and C_2 are temperature (K), the gas constant (8.314 J.K^{-1}.mol^{-1}), the quantity of methylene blue dye adsorbed per unit mass of adsorbent and the concentration of methylene blue dye in aqueous phase, respectively. The linier plot of ln K_C versus 1000/T was used to determine of ΔS and ΔH which calculated from the slope and intercept. The positive value of ΔS indicates that the increase in randomness of ongoing process. The negative value of ΔH indicates that the adsorption process is exothermic in nature and otherwise, the positive value of ΔH indicates that the adsorption process is endothermic in nature. Furthermore, the value of ΔG was calculated with follow the Equation (17). The feasibility and spontaneity of adsorption process was shown by the negative value of ΔG at each temperature.

3. Results and Discussion

3.1 Physical Properties

The XRF results show that the SCEC and TiO_2/SCEC adsorbents consist of major elements, such as: calcium (Ca), silicon (Si), manganese (Mn), and molybdenum (Mo). Many transition metals elements also were found inside the both adsorbents like ferum (Fe), copper (Cu), nickel (Ni), and zinc (Zn). The effect of sulfonation process onto CEC was indicated by percentage of sulfur (9.0%) and it decreases after titanium impregnation process. The percentage of titanium into TiO_2/SCEC adsorbents reach 73.30% after impregnation process by titanium(IV) isopropoxide (500 µmol, Aldrich). The complete list of elements is displayed in Table 1.

Figure 2 shows the FTIR spectra for (a) CEC, (b) SCEC, and (c) TiO_2/SCEC. The O–H stretching mode of the –COOH and phenolic OH groups on the samples were indicated by the broad band at 3416 cm^{-1} in the FTIR spectra [37]. The C–H (aliphatic) stretching vibration in the sample was investigated by the adsorption peaks at 2926 and 2851 cm^{-1}. The vibration band at 1626 cm^{-1} indicates as the adsorption peak of aromatic C=C stretching mode

Table 1. Elements analysis of SCEC and TiO_2/SCEC adsorbent by using XRF.

Sample	Element concentration (wt%)														
	Si	P	S	K	Ca	Ti	Mn	Fe	Ni	Cu	Zn	Br	Mo	Eu	Yb
SCEC	2.90	1.00	9.00	1.2	48.70	0.33	4.49	2.40	0.20	0.48	0.27	1.20	25.00	0.40	0.40
TiO_2/SCEC	1.10	0.55	3.40	0.35	11.10	73.30	1.50	0.81	0.05	0.22	0.19	0.60	6.10	0.20	0.30

Copyright © 2020, BCREC, ISSN 1978-2993

in polyaromatics. The respective intensity of O−H, C–H, and C=C vibration decrease after sulfonation and TiO_2 impregnation onto CEC. The effect of sulfonation process on the adsorbent was proven by the attachment of $–SO_3H$ groups which indicated by the adsorption band at 1177 and 605 cm^{-1} [38]. The effect of titanium impregnation on the adsorbent can be proven by the peak at around 482 cm^{-1} is attributed symmetric O−Ti−O stretching that caused the vibration of Ti−O bond.

The low crystallinity of CEC, SCEC, and TiO_2/SCEC adsorbent were shown by the XRD pattern in Figure 3. The broad peak at 2θ value of 10–30° (C (002)) attributed to amorphous carbon composed of aromatic carbon sheets, can be observed in all adsorbents [37,39,40]. Base on JCPDS number 41-1487, a diffraction peak at 2θ value of 35–50° C (101) indicated that all adsorbents formed turbostratic graphite structure [37,41]. Base on JCPDS number 00-004-0477, the crystal structure of TiO_2 can be observed from the dominant peaks at 25.4° and other peaks at 2θ = 37.9, 48.1, 54.1 and 55.2° but does not appear in Figure 3 (c) due to the amount of titania that added onto SCEC very small (500 µmol).

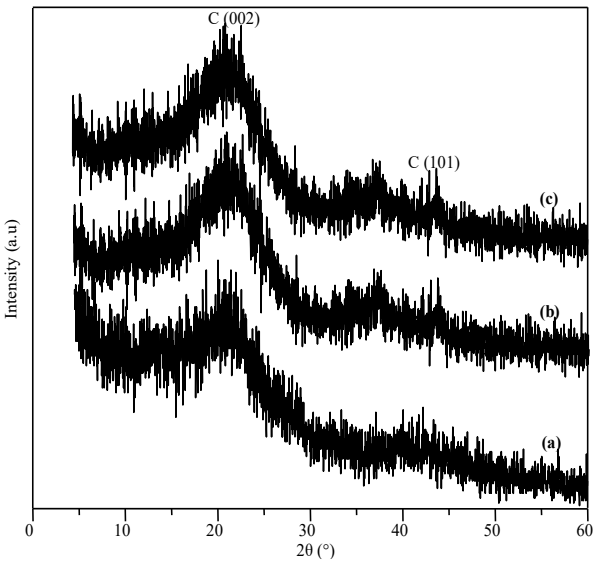

Figure 3. XRD pattern of (a) CEC, (b) SCEC and (b) TiO_2/SCEC adsorbent.

The investigation of weight loss in the TiO_2/SCEC adsorbent which used to control the amount of carbon while increasing the temperature can be shown from the TGA and DTA curves in Figure 4. The weight loss of the adsorbent was obtained in one step. The amount of carbon (18 mg) lose when the temperature increase start at 0 °C, reached midpoint at 400 °C and continued until 800 °C.

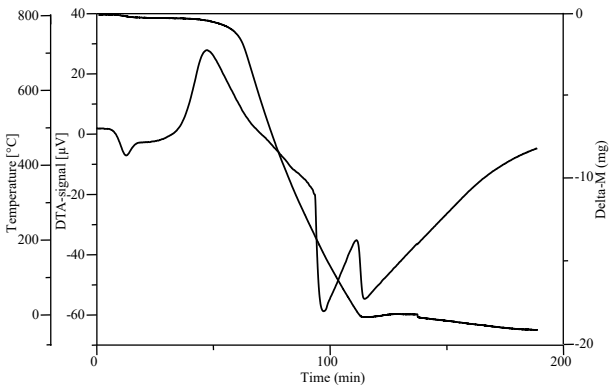

Figure 4. TGA and DTA curves of TiO_2/SCEC adsorbent.

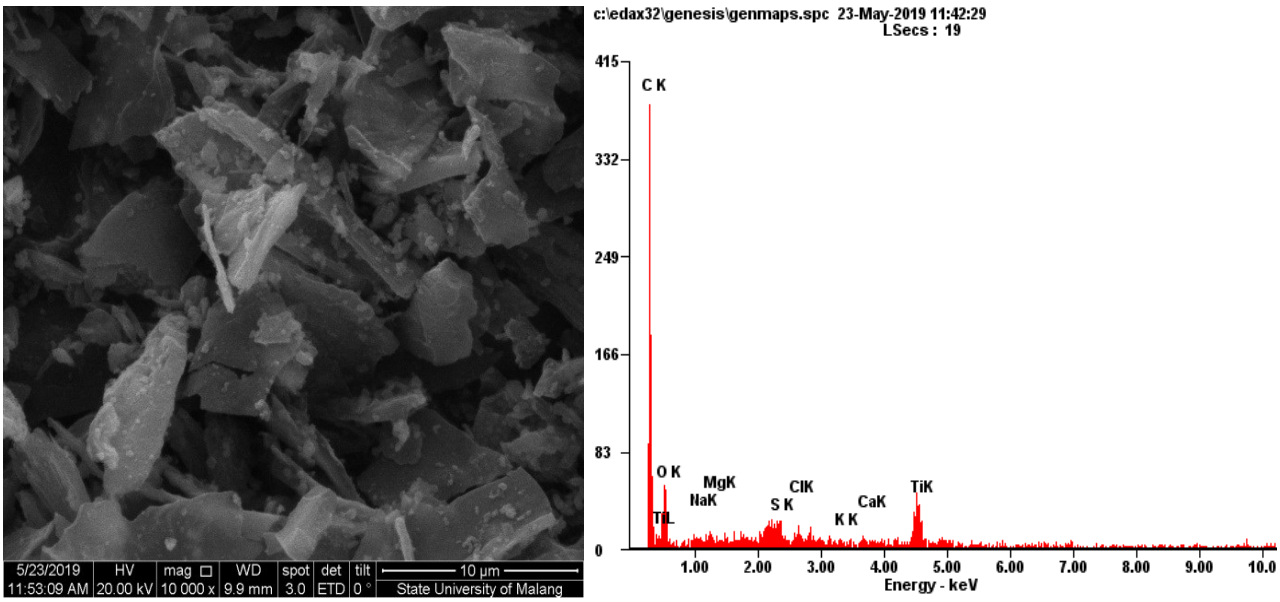

Figure 5. SEM/EDX Image of TiO_2/SCEC adsorbent.

Copyright © 2020, BCREC, ISSN 1978-2993

The SEM image of TiO_2/SCEC adsorbent was shown in Figure 5. The SEM image shows that the TiO_2/SCEC adsorbent is in the fiber form, which is arranged as fibrils. Hollow spaces started to appear after the *E. crassipes* was carbonated and sulfonated. The surface morphology of TiO_2/SCEC adsorbent is roughness. The EDX results (Table 2) show that many elements C, O, Na, Mg, S, Cl, K, Ca, and Ti were detected inside TiO_2/SCEC adsorbent. The adsorbent consists of carbon as a major element. The effect of the sulfonation and titania impregnation process onto adsorbent was proven by the S and Ti elements were found inside adsorbent.

The other physical properties the BET surface area, pore volume and mean pore size of CEC, SCEC, and TiO_2/SCEC were obtained from the nitrogen adsorption-desorption analysis. The complete data were shown in Table 3. The BET surface area, pore volume and mean pore size showed the following values; 94.8 $m^2.g^{-1}$, 0.109 $cm^3.g^{-1}$, 2.303 nm for CEC, 97.8 $m^2.g^{-1}$, 0.184 $cm^3.g^{-1}$, 3.770 nm for SCEC and 233.0 $m^2.g^{-1}$, 0.248 $cm^3.g^{-1}$, 2.131 nm for TiO_2/SCEC, respectively. It can be seen that the BET surface area and pore volume increase can be increased by sulfonation process. And BET surface area and pore volume increase drastically when SCEC was modified to be TiO_2/SCEC by impregnation process.

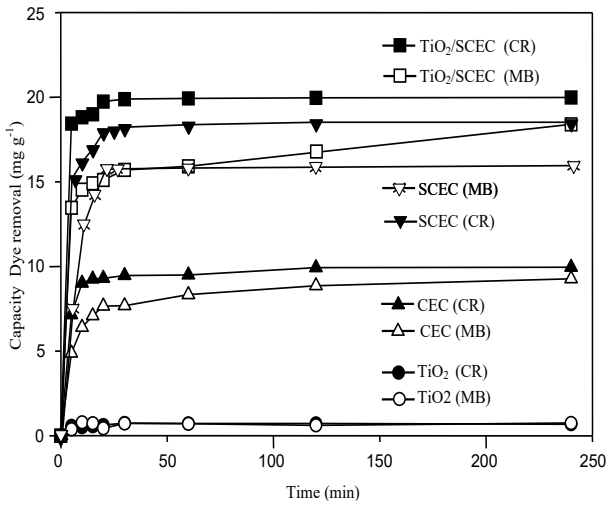

Figure 6. Effect of contact time on the amount of MB and CR dyes removal on TiO_2; CEC, SCEC and TiO_2/SCEC. Conditions: (pH: 6.9, concentration MB and CR 100 $mg.L^{-1}$, weight adsorbent for MB 250 mg and CR 125 mg, at 25°C).

3.2. Effect of Contact Time

The effect of contact time on the dye removal capacity (q_t) of MB and CR onto TiO_2, CEC, SCEC and TiO_2/SCEC adsorbents are shown in Figure 6. TiO_2, CEC, and SCEC adsorbents were used as a comparison to TiO_2/SCEC. These results showed the dye removal capacity of all adsorbents to CR higher than MB. The dye removal capacity for MB or CR dye using TiO_2 adsorbent almost the same ~0.7 $mg.g^{-1}$ in adsorption duration time 5 to 240 min. The dye removal capacity of CEC adsorbent for CR reached 7.1 $mg.g^{-1}$ in adsorption duration time 5 min and drastically increased to 9.0 $mg.g^{-1}$ when adsorption duration time 10 min. The equilibrium CR adsorption was reached within 30 min and the CR removal capacity increased with increasing contact time. The MB removal capacity of CEC adsorbent reached 4.8 $mg.g^{-1}$ within adsorption duration time 5 min and increased up to 6.3 $mg.g^{-1}$ after 10 min. Furthermore, after adsorption duration time 120 min the equilibrium MB achieved 8.9 $mg.g^{-1}$. The CR removal capacity of SCEC achieved 15.1 $mg.g^{-1}$ within adsorption duration time 5 min and increased up to 16.1 $mg.g^{-1}$ after 10 min. Then, after adsorption duration time 30 min the equilibrium CR reached ~18 $mg.g^{-1}$. The MB removal capacity of SCEC achieved ~9.6 $mg.g^{-1}$ within adsorption duration time 5 min

Table 2. Physical properties of SEM EDX of the adsorbent.

Element	wt%
C	68.9
O	20.3
Na	0.6
Mg	0.7
S	1.4
Cl	0.8
K	0.2
Ca	0.7
Ti	6.3

Table 3. Physical properties of CEC, SCEC and TiO_2/SCEC adsorbents

Samples	BET surface area (m^2/g)	Pore Volume (cm^3/g)	Mean pore size (mm)
CEC	94.8	0.109	2.302
SCEC	97.78	0.184	3.770
TiO_2/SCEC	233.0	0.248	2.131

Copyright © 2020, BCREC, ISSN 1978-2993

and after 30 min the equilibrium MB ~16 mg.g^{-1} was achieved. The CR removal capacity of TiO_2/SCEC achieved 18.4 mg.g^{-1} within adsorption duration time 5 min and it showed a slight increase of the equilibrium, 19.9 mg g^{-1} after 30 min. The MB removal capacity achieved 7.8 mg.g^{-1} within adsorption duration time 5 min and increased to a certain extent showing that the equilibrium reached 9.9 mg.g^{-1} after 30 min. Base on the effect of contact time show that CEC, SCEC and TiO_2/SCEC adsorbents more easy to adsorb CR than MB dyes. The sulfonation process onto CEC and impregnation TiO_2 onto SCEC support give positive effect to increase the dye removal capacity which was proven by the dye removal capacity of TiO_2/SCEC > SCEC > CEC > TiO_2 for both dyes. The increasing dye removal capacities were caused by the increasing surface area.

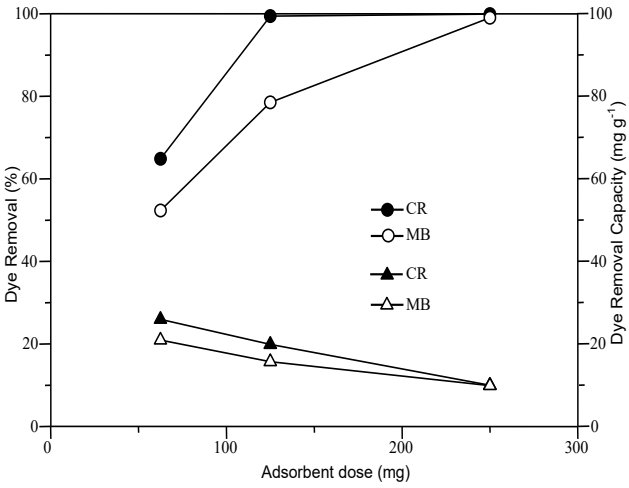

Figure 7. Effect of TiO_2/SCEC adsorbent dose on sorption of MB and CR. Conditions: (pH: 6.9, concentration MB and CR from 100 mg L^{-1}, time 30 min, weight adsorbent: 62.5, 125 and 250 mg, at 25°C).

3.3. Effect of Dose

The plot between the adsorbent dose (mg) versus the percentage of dye removal and dye removal capacity was shown in Figure 7. In this experiment, the dye removal capacity decreased from 20.93 to 9.9 mg.g^{-1} for MB and 25.94 to 9.99 mg.g^{-1} for CR when adsorbent dose has increased from 62.5 to 250 mg. An increase in the dose of adsorbent is not necessary followed by an increase of the dye removal capacity owing to the ratio adsorbent dose to dye concentration is high causing the amount of active sites remaining not covered by dye molecules also high. This result almost in line with the previous research that investigated methylene blue adsorption onto activated carbon prepared from cashew nut shell [3]. The adsorbent dose optimum was achieved 250 mg for MB and 125 mg for CR when the percentage dyes removal almost ~100% for both dyes.

3.4 Effect of pH

The effect of pH on the MB and CR dyes adsorption onto TiO_2/SCEC adsorbent was shown in Figure 8. The removal of MB dye from aqueous solution was effective in the pH range of 2–7. The removal of MB at pH less than 2 was ineffective as the effect of the excess H^+ ion that may caused competition between the positively

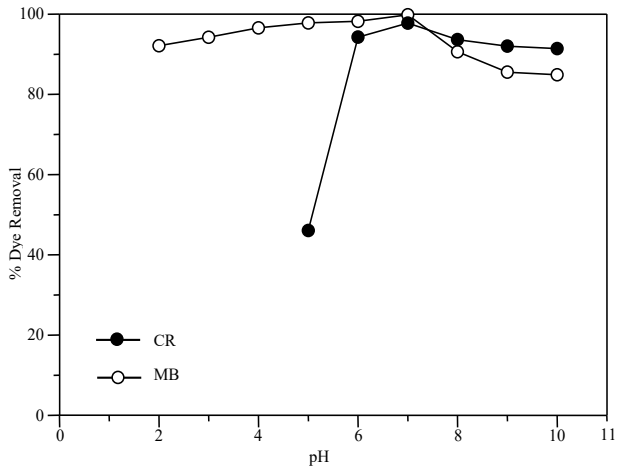

Figure 8. Effect of pH on % MB and CR dye removal on TiO_2/SCEC, Conditions: (pH: 6.9, concentration MB and CR from 100 mg.L^{-1}, weight adsorbent for MB 250 mg and CR 125 mg, at 25°C).

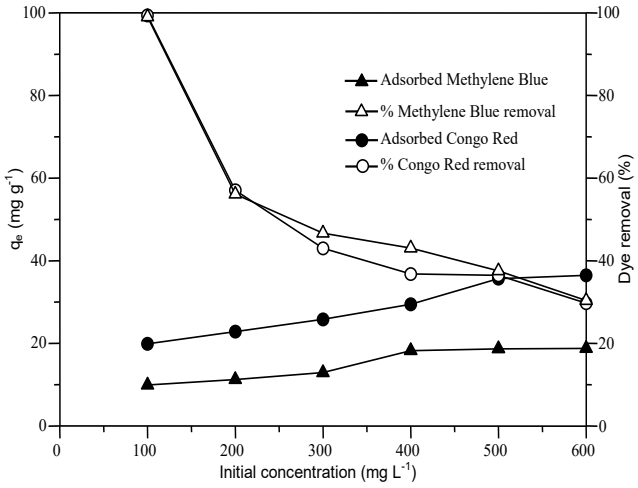

Figure 9. Effect of initial dye concentration on sorption of MB and CR on TiO_2/SCEC. Conditions: (pH: 6.9, concentration MB and CR from 100–600 mg.L^{-1}, weight adsorbent for MB 250 mg and CR 125 mg, at 25°C).

Copyright © 2020, BCREC, ISSN 1978-2993

charged sites (H^+) and the dye$^+$ in adsorption process. The removal of MB tends to decrease due to the excess of the number of negatively charged sites (OH^-) at pH value more than 8 [3]. Otherwise, the CR removal was beneficial in the pH range of 6–10. The removal of CR was not effective at pH less than 5.

3.5 Effect of Initial Concentration

The effect of different initial MB and CR dyes concentrations on the adsorption process is shown in Figure 9. The dyes removal capacity of both dyes increased when the initial concentration increased. At equilibrium, the MB removal capacity increased from 9.9 to 18.8 mg.g^{-1} and the CR removal capacity 19.9 to 36.4 mg.g^{-1} when the initial concentration of both dyes increased from 100 to 600 mg.L^{-1}. The increasing of the amount of dye removal at equilibrium condition was caused by an increasing the initial concentration that can increase the driving force to reduce all mass transfer resistances of the MB and CR dyes molecules between the aqueous and solid phase of the adsorbent [2]. Otherwise, the percentage of both dyes adsorbed decrease from 99.0 to 30.4% for MB and 99.4 to 29.7% for CR when the initial concentration increased from 100 to 600 mg.L^{-1}.

3.6 Adsorption Isotherms

The Langmuir and the Freundlich adsorption isotherms were used to describe the interaction between the dyes and the TiO_2/SCEC adsorbent shown in Figure 10 and 11, respectively. For the removal of MB and CR red by TiO_2/SCEC adsorbent, 25 mL of various dyes concentrations (between 100 and 600 mg.L^{-1}) were mixed with 0.250 mg sorbent for MB and 0.125 g sorbent for CR, then stirred at 300 rpm for 30 min at room temperature. The results are shown in Table 4.

From the Langmuir isotherm can be obtained the value of the constants of Q_{max}, b and R^2 as 36.5 mg.g^{-1}, 2.74×10^{12} and 1.000 for CR and 18.8 mg.g^{-1}, 2.66×10^{12} and 1.000 for MB, respectively. Base on the value of maximum adsorption capacity (Q_{max}), bonding energy (b) can be used to conclude that adsorption of CR was easier than MB onto TiO_2/SCEC adsorbent.

The constant K_F, n, and R^2 were determined from the Freundlich isotherm was obtained 0.2017, 1.002, and 1.000 for CR and 0.1002, 1.001, and 1.000 for MB, respectively. Base on K_F value shows that the MB and CR adsorption process was the heterogeneous adsorption process on the surface of on TiO_2/SCEC adsor-

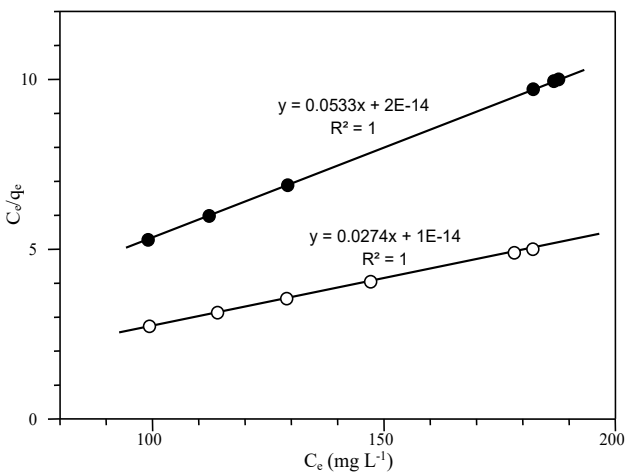

Figure 10. The Langmuir isotherm of MB and CR onto TiO_2/SCEC.

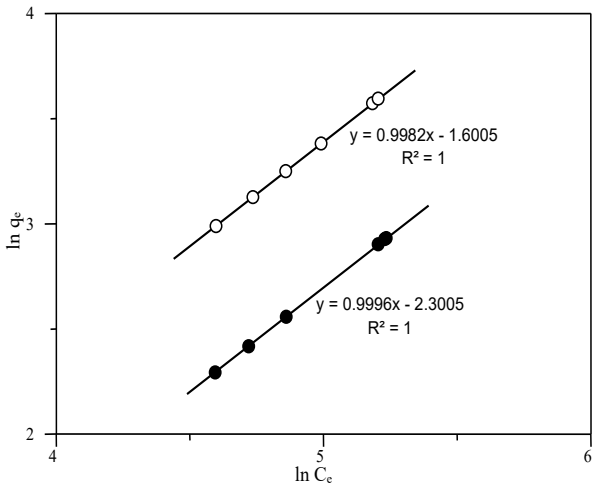

Figure 11. The Freundlich isotherm of MB and CR onto TiO_2/SCEC.

Table 4. Langmuir and Freundlich Isotherm models for CR and MB dyes adsorption on TiO_2/SCEC adsorbent.

Dye removal	Langmuir Isotherm			Freundlich Isotherm		
	Q_o	b	R^2	K_F	n	R^2
Congo Red (CR)	36.5	2.74×10^{12}	1.000	0.2017	1.002	1.000
Methylene Blue (MB)	18.8	2.66×10^{12}	1.000	0.1002	1.001	1.000

Copyright © 2020, BCREC, ISSN 1978-2993

bent which was done through a multi-layer adsorption mechanism. The n values of MB and CR adsorption process are more than 1, which indicates favorable adsorption of both dyes onto the TiO_2/SCEC adsorbent.

3.7 Effect of Particle Size

The effect of adsorbent particle size on dyes removal capacity is shown in Figure 12. The effect of TiO_2/SCEC particle size batch contact experiments were carried out with three particles sizes using adsorbent mass 250 mg for MB and 125 mg for CR, the same initial concentration 100 mg.L^{-1}, and at room temperature. Three selected particle size that used in this experiment 40–100, 100–200 and >200 mesh. The dyes removal capacity were 8.5, 8.7, and 9.9 mg.g^{-1} for MB and 15.9, 16.4, and 19.7 mg.g^{-1} for CR, using the above mentioned particle sizes, respectively. It is worth noting that the dyes removal capacity decreased with an increase in particle size of TiO_2/SCEC adsorbent. This phenomenon can be explained by the smaller particles size for the same amount of adsorbent has larger total surface area [27]. This experiment result was similar with the previous research done on adsorption of Congo red from aqueous solution using roots of *E. crassipes* [16].

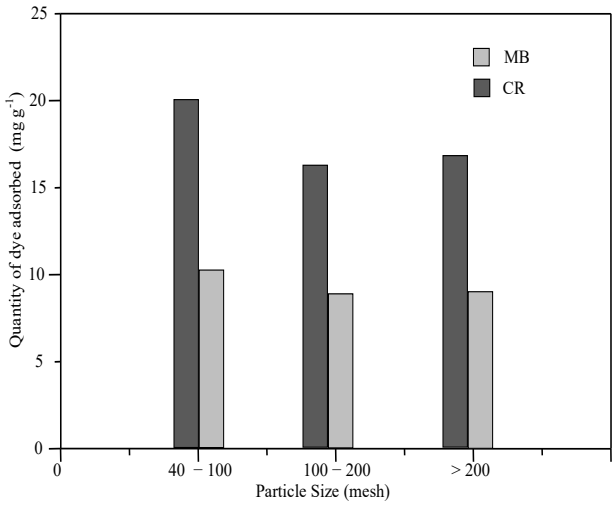

Figure 12. Effect of particle size of adsorbent on the removal of MB and CR dyes (mg.g^{-1}) on TiO_2/SCEC. Conditions: (pH: 6.9, concentration MB and CR from 100 mg.L^{-1}, weight adsorbent for MB 250 mg and CR 125 mg, at 25°C).

3.8 Effect of Temperature

The effect of temperature on the dye removal capacity is shown in Figure 13. The dyes removal capacity at varying temperatures increased from 9.75 to 9.92 mg.g^{-1} (at room temperature), 9.84 to 9.96 mg.g^{-1} (at 40 °C) and 9.91 to 9.98 mg.g^{-1} (at 50°C) for MB and 18.44 to 19.92 mg.g^{-1} (at room temperature), 19.19 to 19.91 mg.g^{-1} (at 40 °C) and 19.46 to 19.98 mg.g^{-1} (at 50 °C) for CR. It can be clearly seen that by increasing the temperature, the dye removal capacity of both dyes also increased slowly and reached optimum at almost 9.98 mg.g^{-1} for MB and 19.98 mg.g^{-1} for CR, respectively. The increasing of dye removal capacity when the adsorption temperature increase was as evident that the adsorption of both dyes onto TiO_2/SCEC adsorbent was endothermic in nature.

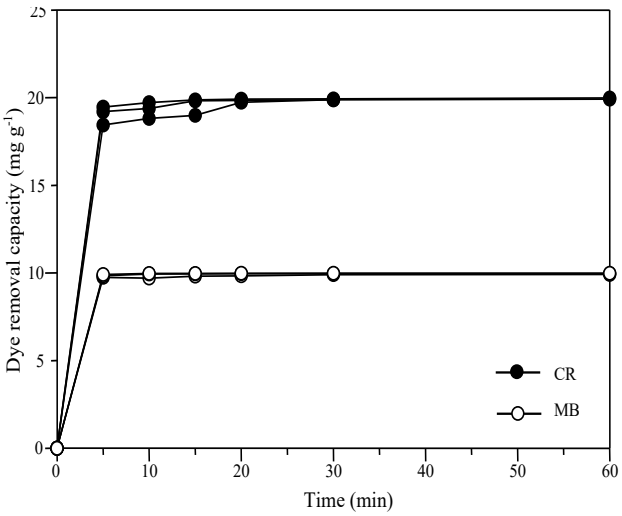

Figure 13. Effect of temperature on on the removal of MB and CR dyes (mg.g^{-1}) on TiO_2/SCEC. Conditions: (pH: 6.9, concentration MB and CR from 100 mg.L^{-1}, weight adsorbent for MB 250 mg and CR 125 mg, at 25, 40, and 50 °C).

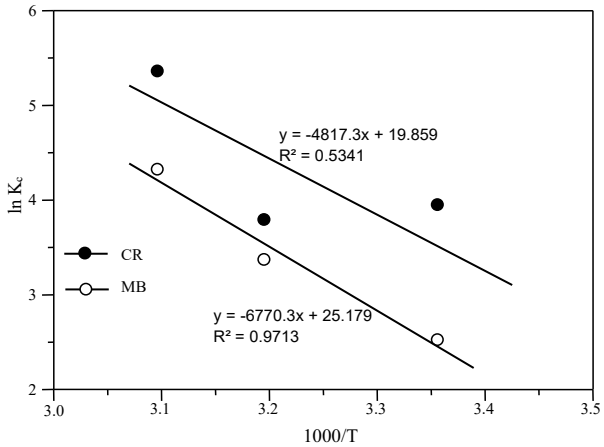

Figure 14. Van't Hoff's plots, ln *K*c vs. 1000/*T* for CR and MB dyes adsorption on TiO_2/SCEC adsorbent

Copyright © 2020, BCREC, ISSN 1978-2993

Figure 14 shows Van't Hoff's plots that used to determine the thermodynamic parameter value of free energy (ΔG), enthalpy (ΔH), and entropy (ΔS). The ΔH and ΔS are calculated based on the slope and intercept. Furthermore, ΔH and ΔS were used to determine ΔG according to equation (17). The values of ΔH, ΔS were +56.56 kJ.mol^{-1}, +0.229 kJ.mol^{-1}.K^{-1} for MB and +40.05 kJ.mol^{-1}, +0.178 kJ.mol^{-1} K^{-1} for CR, respectively. The average values of ΔG were –14.84 kJ.mol^{-1} for MB and –15.52 kJ.mol^{-1} for CR. Positive value of ΔH indicates that the adsorption process of both dyes onto TiO_2/SCEC adsorbent was endothermic in nature. The increasing in degree of system irregularities was identified by the positive value of ΔS. The feasibility and spontaneity of ongoing dyes adsorption process onto TiO_2/SCEC adsorbent was shown by the negative value of ΔG. The complete data of the thermodynamic parameters are listed in Table 5.

3.9 Adsorption of Kinetic

The kinetics data obtained from MB and CR dyes adsorption experiment onto TiO_2/SCEC adsorbent were investigated using pseudo-first-order and pseudo-second order kinetics models. The complete results are given in Table 6. Base on the experiment results, the dyes removal onto TiO_2/SCEC adsorbent at temperature from 25 to 50 °C did not obey a first-order reaction model due to the correlation coefficients R^2<< 1.000 and the dyes removal capacity calculated ($q_{e,cal}$) << the dyes removal capacity experimental ($q_{e,exp}$ = 9.976 mg.g^{-1} for MB; 19.956 mg.g^{-1} for CR).

Otherwise, the parameters kinetic models in Table 6 showed good compliance with the pseudo-second order. This was proven by the correlation coefficients (R^2) for linear plots for MB and CR removal on to TiO_2/SCEC adsorbent were 1.000. The rate constant (k_2) value of the removal of the dyes onto TiO_2/SCEC adsorbent increased with increasing temperature for both dyes. This phenomenon is in line with previous researches that have been reported in the reference for different adsorbate dyes [42]. The highest rate constant of pseudo-second order was found to be 3.7110 for MB and 0.3608 for CR at 50 °C. The calculated ($q_{e,cal}$) and experimental ($q_{e,exp}$) dyes removal capacity at 50 °C were found to be 9.990 and 9.986 mg.g^{-1} for MB and 20.004 and 19.981 mg.g^{-1} for CR. This data indicated that the dyes removal capacity calculated ($q_{e,cal}$) was close to the dyes removal capacity experimental ($q_{e,exp}$). The same phenomenon was found in experiments at 25 °C and 40 °C. The experimental data for dyes removal onto on to TiO_2/SCEC adsorbent fit the pseudo-second order kinetic model. Similar kinetic applications were also determined for dyes removal from aqueous solution with activated carbon produced from tea seed shells 36], activated carbon from cashew nut shell [3], in which the adsorption rate of dyes removal were described by a pseudo-second order.

Table 5. Thermodynamic parameters data for CR and MB dyes adsorption on TiO_2/SCEC adsorbent

Dyes	ΔH (kJ/mol)	ΔS (kJ/mol K)	ΔG (kJ/mol)			Ea (kJ/mol)
			25 °C	40 °C	50 °C	
MB	+56.564	+0.229	−11.779	−15.219	−17.513	82.9
CR	+40.051	+0.178	−13.137	−15.814	−17.599	33.4

Table 6. First order and Pseudo second order kinetics and Freundlich isotherm constants for CR and MB dyes adsorption on TiO_2/SCEC adsorbent.

Dye removal	Temperature (°C)	First Order			Pseudo Second Order			$q_{e,exp}$ (mg.g^{-1})
		$q_{e,cal}$ (mg.g^{-1})	k_1 (g.mg^{-1}.h^{-1})	R^2	$q_{e,cal}$ (mg.g^{-1})	k_2 (g.mg^{-1}.h^{-1})	R^2	
Congo Red (CR)	25	0.932	0.0371	0.7851	20.000	0.1276	1.000	19.976
	40	1.153	0.1226	0.8717	20.000	0.2475	1.000	19.910
	50	0.636	0.0953	0.8887	20.004	0.3608	1.000	19.981
Methylene Blue (MB)	25	0.540	0.0295	0.5640	9.980	0.2997	1.000	9.976
	40	0.123	0.1451	0.9729	9.920	2.3090	1.000	9.965
	50	0.143	0.1728	0.9456	9.990	3.7110	1.000	9.986

Copyright © 2020, BCREC, ISSN 1978-2993

4. Conclusions

Many research using *E. crassipes* as the raw material of adsorbents to remove dyes have been conducted. In this work, the *E. crassipes* is a tropical plant, which is low in cost and abundant elsewhere. Therefore, it was chosen as an alternative, natural source of carbon and followed by sulfonation and titania impregnation to be an adsorbent. The batch system was used for the adsorption process of MB and CR onto TiO_2/SCEC at initial concentration of 100 mg/L at room temperature. The TiO_2/SCEC adsorbent exhibited higher removal capacity toward MB and CR dyes. The experiment data indicated that the adsorption kinetics of dyes onto the TiO_2/SCEC followed pseudo-second order model. The parameters thermodynamic data indicated the dyes adsorption process onto the TiO_2/SCEC was endothermic and spontaneous in nature. Results showed the removal of CR more effective than MB onto the TiO_2/SCEC adsorbent.

Acknowledgements

The authors gratefully acknowledge research grant from IsDB TA. 2019, (No: 137/UN17.11/PL/2019) and education faculty and teaching training Mulawarman University, East Kalimantan Province, Indonesia.

References

[1] Mahmoodi, N.M., Salehi, R., Arami, M. (2011). Binary system dye removal from colored textile wastewater using activated carbon: Kinetic and isotherm studies. *Desalination*, 272, 187-195. DOI: 10.1016/j.desal.2011.01.023.

[2] Wanyonyi, W.C., Onyari, J.M., Shiundu, P.M. (2013). Adsorption of Methylene Blue Dye from Aqueous Solution Using Eichhornia crassipes. *Bull. Environ. Contam. Toxicol.*, 91(3), 362-366. DOI: 10.1007/s00128-013-1053-0.

[3] Kumar, P.S., Ramalingam, S., Sathishkumar, K. (2011). Removal of methylene blue dye from aqueous solution by activated carbon prepared from cashew nut shell as a new low-cost adsorbent. *Korean J. Chem. Eng.,* 28(1), 149-155. DOI: 10.1007/s11814-010-0342-0.

[4] Nigam, P., Armour, G., Banat, I.M., Singh, D., Marchant, R. (2000). Physical removal of textile dyes from effluents and solid-sate fermentation of dye-adsorbed agricultural residues. *Bioresour. Technol.*, 72, 219-226. DOI: 10.1016/S0960-8524(99)00123-6.

[5] Wawrzkiewicz, M., Polska-Adach, E., Hubicki, Z. (2019). Application of titania based adsorbent for removal of acid, reactive and direct dyes from textile effluents. *Adsorption,* 25, 621–630. DOI: 10.1007/s10450-019-00062-0.

[6] Hachem, C., Bocquillon, F., Zahraa, O., Bouchy, M. (2001). Decolourization of textile industry wastewater by the photocatalytic degradation process. *Dyes and Pigments,* 49, 117-125. DOI: 10.1016/S0143-7208(01)00014-6.

[7] Park, C., Lee, M., Lee, B., Kim, S.-W., Chase, H.A., Lee, J., Kim, S. (2007). Biodegradation and biosorption for decolorization of synthetic dyes by Funalia trogii. *Biochem. Eng. J.,* 36, 59-65. DOI: 10.1016/j.bej.2006.06.007.

[8] Crini, G. (2006). Non-conventional low-cost adsorbents for dye removal: A review, *Bioresour. Technol.,* 97, 1061-1085. DOI: 10.1016/j.biortech.2005.05.001.

[9] Alinsafi, A., Khemis, M., Pons, M. N., Leclerc, J. P., Yaacoubi, A., Benhammou, A., Nejmeddine, A. (2005). Electro-coagulation of reactive textile dyes and textile wastewater. *Chem. Eng. Process.,* 44, 461-470. DOI: 10.1016/j.cep.2004.06.010.

[10] Karaoglu, M.H., Dogan, M., Alkan, M. (2010). Removal of Reactive Blue 221 by Kaolinite from Aqueous Solution. *Ind. Eng. Chem. Res.,* 49, 1534-1540. DOI: 10.1021/ie9017258.

[11] Peng, Q., Yu, F., Huang, B., Huang, Y. (2017). Carbon-containing bone hydroxyapatite obtained from tuna fish bone with high adsorption performance for Congo red. *The Royal Soc. Chem.,* 17, 26968. DOI: 10.1039/C6RA27055G

[12] Wang, L. (2012). Application of activated carbon derived from waste bamboo culm for the adsorption of azo disperse dye: kinetic, equilibrium and thermodynamic studies. *J. Environ. Manag.,* 102, 79-87. DOI: 10.1016/j.jenvman.2012.02.019.

[13] Kusumawardani, R., Nurhadi, M., Wirhanuddin, Gunawan, R., Nur, H. (2019). Carbon-containing Hydroxyapatite Obtained from Fish Bone as Low-cost Mesoporous Material for Methylene Blue Adsorption. *Bull. Chem. Reac. Eng. Catal., 14*(3), 660-671. DOI: 10.9767/bcrec.14.3.5365.660-671.

[14] Muthukumar, M., Sevakumar, N. (2004). Studies on the effect of inorganic salts on decolouration of acid dye effluent by ozonation. *Dyes and Pigments,* 62, 221-228. DOI: 10.1016/j.dyepig.2003.11.002.

[15] Sikaily, A.E., Khaled, A., Nemr, A.E., Abdelwahab, O. (2006). Removal of Methylene Blue from aqueous solution by marine green alga

Copyright © 2020, BCREC, ISSN 1978-2993

Ulva lactuca. *Chem. Ecol.,* 22, 149-157. DOI: 10.1080/02757540600579607.

[16] Wanyonyi, W.C., Onyari, J.M., Shiundu, P.M. (2014). Adsorption of Congo Red Dye from Aqueous Solution Using Roots of Eichhornia Crassipes: Kinetic and Equilibrium Studies *Energy Procedia,* 50, 862-869. DOI: 10.1016/j.egypro.2014.06.105.

[17] Zawahry, M.M.E., Kamel, M.M. (2004). Removal of azo and anthraquinone dyes from aqueous solutions by Eichhornia Crassipes. *Water Research,* 38, 2967-2972. DOI: 10.1016/S0043-1354(01)00526-7.

[18] Belessi, V., Romanos, G., Boukos, N., Lambropoulou, D., Trapalis, C. (2009). Removal of Reactive Red 195 from aqueous solutions by adsorption on the surface of TiO_2 nanoparticles. *J. Hazard. Mater.,* 170, 836-844. DOI: 10.1016/j.jhazmat.2009.05.045.

[19] Wang, R., Cai, X., Shen, F. (2014). TiO2 hollow microspheres with mesoporous surface: Superior adsorption performance for dye removal. *Applied Surface Sci.,* 305, 352-358. DOI: 10.1016/j.apsusc.2014.03.089.

[20] Sriprang, P., Wongnawa, S., Sirichote, O. (2014). Amorphous titanium dioxide as an adsorbent for dye polluted water and its recyclability. *J. Sol-Gel Sci. Technol.,* 71, 86-95. DOI: 10.1007/s10971-014-3327-3.

[21] Kamal, T., Anwar, Y., Khan, S. B., Chani, M. T. S., Asiri, A. M. (2016). Dye adsorption and bactericidal properties of TiO2/chitosan coating layer. *Carbohydrate Polym.,* 148, 153-160. DOI: 10.1016/j.carbpol.2016.04.042.

[22] Li, J., Feng, J., Yan, W. (2013). Synthesis of Polypyrrole-Modified TiO_2 Composite Adsorbent and Its Adsorption Performance on Acid Red G. *J. Appl. Polym. Sci.,* 128, 3231–3239. DOI: 10.1002/app.38525.

[23] Nurhadi, M., Widiyowati, I. I., Wirhanuddin, Chandren, S. (2019). Kinetic of Adsorption Process of Sulfonated Carbon-derived from Eichhornia crassipes in the Adsorption of Methylene Blue Dye from Aqueous Solution, *Bull. Chem. Reac. Eng. Catal.,* 14(1), 17-27. DOI: 10.9767/bcrec.14.1.2548.17-27.

[24] Ito, S., Kon, Y., Nakashima, T., Hong, D., Konno, H., Ino, D., Sato, K. (2019). Titania-Catalyzed H_2O_2 Thermal Oxidation of Styrenes to Aldehydes. *Molecules,* 24, 1-9. DOI: 10.3390/molecules24142520.

[25] Pathania, D., Arush, S., Siddiqi, Z.M., (2016). Removal of congo red dye from aqueous system using Phoenix dactylifera seeds. *J. Mol. Liq.,* 219, 359-367. DOI: 10.1016/j.molliq.2016.03.020.

[26] Yahong, Z., Zhenhua, X., Ximing, W., Li, W., Aiqin, W. (2012). Adsorption of Congo Red onto Lognocellulose/Montmorillonite Nanocomposite. *J. Wuhan University Technol. Mater.,* 27(5), 931-938. DOI: 10.1007/s11595-012-0576-2.

[27] Aksu, Z., (2005). Application of biosorption for the removal of organic pollutants: a review, *Process Biochem.*, 40, 997-1026. DOI: 10.1016/j.procbio.2004.04.008.

[28] Lima, H.K., Tenga, T.T., Ibrahima, M.H., Ahmad, A., Chee, H.T. (2012). Adsorption and Removal of Zinc(II) from Aqueous Solution Using Powdered Fish Bones. *APCBEE Procedia,* 1, 96 – 102. DOI: 10.1016/j.apcbee.2012.03.017.

[29] Mohanty, K., Jha, M., Meikap, B.C., Biswas, M.N. (2006). Biosorption of Cr(IV)from aqueous solutions by Eichhornia crassipes. *Chem. Eng. J.,* 117, 71-77. DOI: 10.1016/j.cej.2005.11.018.

[30] Mahmoodi, N.M., Kharramfar, S., Najafi, N. (2011). Amine-functionalized silica nanoparticle:Preparation, characterization and anionic dye removal ability. *Desalination,* 279, 61-68. DOI: 10.1016/j.desal.2011.05.059.

[31] Ho, Y.S., McKay, G. (1999). Pseudo-second order model for sorption processes. *Process Biochem.,* 34, 451-465. DOI: 10.1016/S0032-9592(98)00112-5.

[32] Yang, L., Zhang, Y., Liu, X., Jiang, X., Zhang, Z., Zhang, T., Zhang, L. (2014). The Investigation of Synergistic and competitive interaction between dye Congo red and Methyl blue on magnetic $MnFe_2O_4$. *Chem. Eng. J.*, 246, 88-96. DOI: 10.1016/j.cej.2014.02.044.

[33] Khaniabadi, Y.O., Basiri, H., Nourmoradi, H., Mohammadi, M.J., Yari, A.R., Sadeghi, S., Amrane, A. (2017). Adsorption of Congo Red Dye From Aqueous Solutions by Montmorillonite as a Low-cost Adsorbent. *Inter. J. Chem. React. Eng.,* 16(1), 1-11. DOI: 10.15171/EHEM.2017.05.

[34] Sharma, P.K., Ayub, S., Tripathi, C.N. (2016). Isotherm describing physical adsorption of Cr(VI) from aqueous solution using various agricultural wastes as adsorbent. *Cogent. Eng.,* 3, 1-20. DOI: 10.1080/23311916.2016.1186857.

[35] Baccar, R., Blangquez, P., Bouzid, J., Feki, M., Sarra, M. (2010). Equilibrium, thermodynamic and kinetic studies on adsorption of commercial dye by activated carbon derived from olive-waste cakes. *Chem. Eng. J.,* 165(2), 457-464. DOI: 10.1016/j.cej.2010.09.033.

[36] Gao, J.-J., Qin, Y.-B., Zhou, T., Cao, D.-D., Xu, P., Hochstetter, D., Wang, Y.-F. (2013). Adsorption of methylene blue onto activated carbon produced from tea (Camellia sinensis

Copyright © 2020, BCREC, ISSN 1978-2993

L.) seed shells: kinetics, equilibrium, and thermodynamics studies. *J.f Zhejiang University: Science B (Biomedicine & Biotechnol.),* 14(7), 650-658. DOI: 10.1631/jzus.B12a0225.

[37] Nurhadi, M., Chandren, S., Yuan, L. S., Ho, C. S., Mahlia, T. M. I., Nur, H. (2017). Titania-Loaded Coal Char as Catalyst in Oxidation of Styrene with Aqueous Hydrogen Peroxide. *Int. J. Chem. Reactor Eng.*, 15(1), 1-11. doi: 10.1515/ijcre-2016-0088.

[38] Geng, L., Wang, Y., Yu, G., Zhu, Y. (2011). Efficient carbon-based solid acid catalysts for the esterification of oleic acid. *Catal. Commun.*, 13(1), 26-30. DOI: 10.1016/j.catcom.2011.06.014.

[39] Nurhadi, M., Kusumawardani, R., Nur, H. (2018). Negative Effect of Calcination to Catalytic Performance of Coal Char-loaded TiO_2 Catalyst in Styrene Oxidation with Hydrogen Peroxide as Oxidant. *Bull. Chem. Reac. Eng. Catal.*, *13*(1), 113-118. DOI: 10.9767/bcrec.13.1.1171.113-118.

[40] Nurhadi, M. (2017). Modification of Coal Char-loaded TiO_2 by Sulfonation and Alkylsilylation to Enhance Catalytic Activity in Styrene Oxidation with Hydrogen Peroxide as Oxidant. *Bull. Chem. Reac. Eng. Catal.,* 12(1), 55-61. DOI: 10.9767/bcrec.12.1.501.55-61.

[41] Peng, L., Philippaerts, A., Ke, X., Van Noyen, J., De Clippel, F., Van Tendeloo, G., Sels, B.F. (2010). Preparation of sulfonated ordered mesoporous carbon and its use for the esterification of fatty acids. *Catal. Today,* 150(1–2), 140-146. DOI: 10.1016/j.cattod.2009.07.066.

[42] Qi, Z., Wenqi, G., Chuanxin, X., Dongjiang, Y., Xiaoqing, L., Xiao, Y. Xiaofang, L. (2011). Removal of Neutral Red from aqueous solution by adsorption on spent cottonseed hull substrate. *J. Hazard. Mater.,* 185, 502-506. DOI: 10.1016/j.jhazmat.2010.09.029.

Copyright © 2020, BCREC, ISSN 1978-2993